



# NASA Technical Memorandum 89110

## INTEGRATED STRUCTURE ELECTROMAGNETIC OPTIMIZATION OF LARGE SPACE ANTENNA REFLECTORS

(NASA-TM-89110) INTEGRATED STRUCTURE  
ELECTROMAGNETIC OPTIMIZATION OF LARGE SPACE  
ANTENNA REFLECTORS (NASA) 12 p CSCI 22B

N87-18598

Unclas

G3/18 43615

Sharon L. Padula, Howard M. Adelman,  
and M. C. Bailey

February 1987



# INTEGRATED STRUCTURAL ELECTROMAGNETIC OPTIMIZATION OF LARGE SPACE ANTENNA REFLECTORS

by

S. L. Padula<sup>\*</sup>, H. M. Adelman<sup>\*\*</sup> and M. C. Bailey  
NASA Langley Research Center  
Hampton, Virginia

## Abstract

The requirements for extremely precise and powerful large space antenna reflectors have motivated the development of a procedure for shape control of the reflector surface. A mathematical optimization procedure has been developed which improves antenna performance while minimizing necessary shape correction effort. In contrast to previous work which proposed controlling the rms distortion error of the surface thereby indirectly improving antenna performance, the current work includes electromagnetic (EM) performance calculations as an integral part of the control procedure. The application of the procedure to a radiometer design with a tetrahedral truss backup structure demonstrates the potential for significant improvement. The results indicate the benefit of including EM performance calculations in procedures for shape control of large space antenna reflectors.

## Nomenclature

G	maximum power density for distorted antenna
$G_0$	maximum power density for undistorted antenna
$\Delta l$	vector of actuator length changes
$\Delta l_{max}$	maximum change in actuator length
m	number of shape control actuator locations
n	number of joints between truss elements on reflector surface
rms	root mean square of surface distortion errors
SLL	maximum power density outside the main beam radiation angle (side lobe level)
U	influence matrix used in equation 2
X,Y,Z	Cartesian coordinate system with origin at center of paraboloid (Fig. 1)

z	vector of n surface displacement errors in Z direction
$\beta$	slack variable used to implement optimization procedure
$\theta$	antenna radiation angle measured from the paraboloid axis
$\theta_0$	radiation angle which defines main beam region
$\lambda$	wavelength of electromagnetic radiation
$\phi$	azimuthal angle measuring rotation around the paraboloid axis
$\psi$	vector of random surface displacement errors in the Z direction

## Introduction

In studies of the design and operation of large space reflector antennas, a key issue is the precise shape control of the reflector surface in order to guarantee satisfactory electromagnetic (EM) performance. However, when discussing antenna design criteria, most authors treat the subjects of structural design, shape control, and electromagnetic performance as separate issues.<sup>1-4</sup> The link between the structural deformation and the loss of antenna performance has been based on classical formulas such as that of Ruze (ref.5) in which the antenna performance is related to the rms value of the surface distortion error. Although the rms value of the surface roughness can be used to calculate the gain loss for a slightly distorted reflector antenna, other performance parameters (i.e. beam shape, beam pointing direction, side lobe level and side lobe distribution) depend upon the details of the distortion throughout the reflector surface.

Recently, some initial steps have been taken to integrate the thermal, structural and EM analysis in order to produce a more effective analysis procedure and to account for the relation between details of the distortion and antenna performance.<sup>6-9</sup> The present paper proposes, develops and demonstrates an optimization procedure for shape control of a large space antenna (LSA) reflector. The main feature which distinguishes this work from previous efforts is that the shape control mechanism is driven by the need to satisfy explicit EM design requirements rather than implicit limits on rms surface accuracy.

\* Member AIAA  
\*\* Member AIAA, ASME

The optimization procedure is tested by applying it to a specific antenna configuration which was designed for a microwave radiometer mission. A radiometer design is attractive because remote sensing is a driving force behind NASA interest in LSA systems and because the constraints on electromagnetic performance are both critical and difficult to achieve.

In the present work, the radiometer surface shape is controlled by a set of actuators which can lengthen or shorten individual members of the backup structure. The optimization procedure must select a set of actuator inputs which smooths the reflector surface enough to satisfy EM performance criteria while minimizing the total actuator effort required. It is shown that the general purpose procedure is effective when applied to a typical surface distortion on a particular antenna reflector design. Moreover, it is shown that the procedure is much more effective than the technique of merely reducing rms surface distortion.

### Structural Shape Control

This section describes the application of shape control to a tetrahedral truss antenna structure similar to designs developed for the NASA.<sup>3,4</sup> Figure 1 illustrates the antenna configuration, the finite element model of the reflector support structure and the coordinate system used to analyze the antenna performance. The support structure is a tetrahedral truss fabricated from graphite epoxy tubes. The individual truss members are divided into three groups: those on the top or feed facing surface, those on the bottom surface and those which connect the two surfaces.

The principal source of distortion in the truss is expected to be inaccuracies in the lengths of the individual truss members. The length inaccuracies occur due to manufacturing variations in length or material properties. For example, although the coefficient of thermal expansion of graphite epoxy is very small, the variation in this parameter from member to member can cause distortions in a uniform temperature field. The effect of these length inaccuracies can be determined by performing multiple structural analyses with multiple sets of member length errors selected at random according to an assumed probability density function as in reference 10.

To test the design procedure in this study, a single set of random member lengths was selected and used for all design studies. The errors in member length are assumed to be normally distributed with a mean of zero and a standard deviation of 0.015% of element length. These errors are consistent with the studies in reference 10.

Shape correction of the top surface of the truss structure is similar to the method of applied temperature described in reference 11. A set of  $m$  actuators is positioned on the bottom surface of the truss structure. The action of these actuators is to lengthen or shorten the individual elements to which they are attached.

The best locations for the actuators are found by the method of reference 12.

The net surface shape distortion resulting from member length errors and actuator inputs is computed by a standard finite element structural analysis program, EAL,<sup>13</sup> and measured by comparing the location of the  $n$  joints on the top surface with their ideal locations. If  $z$  is the vector of displacement errors in the  $Z$  direction then the rms surface error is one measure of surface accuracy.

$$rms = \sqrt{\sum_{i=1}^n z_i^2 / n} \quad (1)$$

For any set of actuator inputs,  $\{\Delta l\}$ , the resulting distortion of the feed facing surface can be expressed as

$$\{z\} = \{\psi\} + [U] \{\Delta l\} \quad (2)$$

where  $\{\Delta l\}$  is the vector of changes in length of actuator elements,  $\{\psi\}$  is the original random distortion error vector,  $\{z\}$  is the distortion error after correction and  $[U]$  is an influence matrix. The influence matrix is assembled in EAL such that the  $i$ -th column of  $[U]$  is the displacement of the structure due to a unit change in the  $i$ -th actuator element. Also determined by EAL is the set of actuator inputs  $\{\Delta l\}$  which minimize  $z^T z$  and which therefore produce the minimum rms distortion. This set,  $\{\Delta l\}$ , satisfies the equation

$$[A] \{\Delta l\} = \{r\} \quad (3)$$

$$\text{where } [A] = [U]^T [U]$$

$$\text{and } \{r\} = -[U]^T \{\psi\}$$

While this set of actuator inputs does minimize rms distortion, it may not be the best choice for control of the surface.

### Electromagnetic Characteristics

This section describes the electromagnetic performance characteristics which are used to evaluate the success of the antenna reflector shape control procedure. The electromagnetic analysis in this study was performed by a modification of the NEC-REF<sup>14</sup> reflector antenna code which accounts for the actual surface distortion from the finite element structural analysis. The calculations are obtained by a geometrical optics projection of the feed radiation reflected from the antenna surface onto a plane normal to the axis of the paraboloid. The phase of these fields is then perturbed by the difference in the ray path length caused by the reflector surface distortion. A double numerical Fourier transform of these perturbed fields yields the electromagnetic characteristics of the reflector antenna. The accuracy of the modified NEC-REF code for predicting the radiation patterns of distorted reflector antennas has been previously

verified<sup>15</sup> through comparison with measured results for two mesh reflector antennas.

The electromagnetic radiation characteristics for a perfectly smooth reflector antenna are illustrated by the calculated radiation pattern in figure 2. This pattern is a plot of radiated power density versus the angle,  $\theta$ , measured from the paraboloidal axis. The plot is normalized to the maximum power density, which is referred to as the antenna gain (G). The main beam of the antenna radiation pattern is defined by nulls which occur at  $\theta = \pm\theta_0$ . The maximum side lobe level (SLL) is defined as the highest level of the radiation pattern outside the main beam. The plot in figure 2 is for a particular azimuth angle ( $\phi = 45^\circ$ ). The radiation patterns for other azimuth angles are identical to figure 2.

Figure 3 illustrates the effect of a typical surface distortion on the radiation pattern of the antenna. Patterns for two orthogonal planes ( $\phi = 45^\circ, 135^\circ$ ) are presented which illustrate that the radiation patterns from the distorted antenna are no longer axisymmetric but become a function of azimuth angle.

In a radiometer system, the received power is the integrated electromagnetic emission arriving at the antenna from all angular directions weighted by the antenna radiation pattern. The antenna performance parameter of most importance for a radiometer is the amount of energy received within the main beam relative to that received from all other directions. The relative energy in the main beam is defined as the beam efficiency and is determined by comparing the double integral of the radiation pattern over the main beam with the double integral of the radiation pattern over  $4\pi$  steradians. In an optimization procedure, in which the radiation pattern shape changes for each step of the optimization, the numerical calculation of beam efficiency as a constraint would be prohibitively time consuming. However, since the energy contained in the angular region outside the main beam can be a significant source of error in the interpretation of data for a radiometer system,<sup>16</sup> the maximum level of the radiation pattern for angles greater than  $\theta_0$  will be the primary constraint imposed upon the optimization procedure for the present study. In order to further insure that the antenna beam efficiency remains high, an additional constraint will be imposed upon the decrease in maximum gain compared to the gain for the undistorted antenna ( $G_0$ ).

For other large antenna applications (e.g. communications and radar), the gain and side lobe level are the performance parameters of most importance. Therefore, constraining these parameters in the optimization procedure will also demonstrate the flexibility of the procedure for a wide class of large antenna applications. Several other antenna performance parameters (e.g. polarization purity, beam-pointing direction, and feed-positioning accuracy) will not be constrained in this present study, although, these could be included

in the optimization procedure for an application in which these parameters were of significant concern.

### Optimization Formulation

In this section an optimization procedure is described which will improve the surface accuracy and the resulting electromagnetic performance of the antenna reflector while minimizing the energy used to power the actuators. The design variables for the procedure are the actuator inputs,  $\Delta l$ . The optimization problem is solved using the method of feasible directions as implemented in CONMIN<sup>17</sup>.

The optimization procedure seeks to minimize the maximum actuator input. This objective tends to distribute the corrective force evenly among all of the actuators. Thus, actuators can be sized smaller and lighter and the total amount of power required can be reduced.

The optimization problem is as follows:

$$\text{minimize } |\Delta l_{\max}| \quad (4)$$

$$\text{subject to } \text{SLL} \leq G_0 - 30 \text{ dB}$$

$$G \geq G_0 - 0.3 \text{ dB}$$

$$\text{rms} \leq \lambda/50$$

where  $\Delta l_{\max}$  is the maximum change in length of an actuator element,  $\lambda$  is the wavelength of EM radiation,  $G$  is the antenna gain for the distorted reflector and  $G_0$  is the antenna gain for the ideal reflector.

The primary constraint on EM performance is that the maximum side lobe level (SLL) must be at least 30 decibels below the ideal antenna gain. The added constraint on antenna gain ( $G$ ) means that at least 95 percent of the signal power will be in the main beam of the antenna. The final constraint (on the rms surface distortion error) is included to help the optimization routine eliminate unproductive search directions. The rms error constraint is consistent with the antenna gain constraint for small amounts of distortion (ref 5).

A useful formulation of the optimization problem includes a slack variable,  $\beta$ , as follows:

$$\text{minimize } \beta \quad (5)$$

$$\text{subject to } |\Delta l_i| \leq \beta \quad i=1,2, \dots, m$$

$$\text{SLL} \leq G_0 - 30 \text{ dB}$$

$$G \geq G_0 - 0.3 \text{ dB}$$

$$\text{rms} \leq \lambda/50$$

where  $\Delta l_i$  is the change in length of the  $i$ -th actuator element. This formulation is preferred because the discontinuous objective function  $\Delta l_{\max}$  is replaced by a linear objective function  $\beta$ .

An important aspect of the optimization problem is that the EM constraints and their gradients with respect to the design variables are relatively expensive to compute. Rather than perform a complete EM analysis each time that CONMIN requires a new constraint value, the EM performance measures are calculated once and linear approximations are used thereafter. The finite difference approximation to the gradients of the constraint functions are calculated once as well. The optimization problem is solved with move limits on the design variables, so that the linear approximation will remain valid. When a solution is reached, the actual values of EM performance are calculated at the solution point. If this solution is a feasible one and if the objective function has not changed significantly from the previous value, then the process stops. Otherwise, the constraint gradients are recalculated and the entire process is repeated until an acceptable solution is found.

As discussed in the section on EM characteristics, the NEC-REF code calculates relative power levels at discrete values of  $\theta$  and  $\phi$ . In order to reduce the amount of computation required, SLL is defined as the maximum level found in the range,  $\theta_0 < |\theta| < 4\theta_0$ , for four different values of  $\phi$  which are  $45^\circ$  apart. It is assumed that an antenna surface which reduces the side lobe levels in these four directions will reduce levels in all directions. The constraints on loss of antenna gain and on rms error are added insurance that side lobe levels will decrease in all directions. The consequences of this assumption are discussed in a later section.

#### Test Problem

The optimization procedure is applied to a specific test problem detailed in this section. The problem is constructed by selecting realistic parameter values from tables found in references 3 and 4. The resulting problem has challenging performance criteria but is not a worst case model.

The 55-meter tetrahedral truss reflector, illustrated in figure 1, has a focal length to diameter ratio of 1.5 and an operating frequency of 1.4 GHz. The wavelength,  $\lambda$ , of EM radiation is 8.436 inches. The antenna gain for the ideal antenna,  $G_0$ , is 56.64 dB and the radiation angle defining the main beam,  $\theta_0$ , is 0.5 degrees.

The antenna backup structure is composed of 420 truss elements. The reflective surface is approximated by a spline fit through the 61 joint locations on the top surface of the antenna. The distortion at these 61 discrete points is controlled by 48 actuator elements on the bottom surface of the antenna.

#### Results

In this section, the results of the optimization problem are examined. Starting with zero inputs (ie.  $\Delta l_i = 0$ ), the optimization procedure converges to a feasible

set of inputs which has the lowest possible  $\Delta l_{\max}$ . The entire process requires eleven optimization cycles, that is eleven evaluations of the EM performance measures and their gradients. The success of the method is illustrated by comparing the antenna radiation patterns before and after optimization.

Figure 4 contains a convergence history of the optimization problem. Figure 4a is a plot of the objective function,  $\Delta l_{\max}$ , as a function of optimization cycle number. The problem begins with zero actuator inputs, and they increase until a feasible design is reached. The maximum change in actuator length then decreases smoothly to a final value of .066 inches.

As seen in figures 4b and 4c, the requirement for low side lobe levels is met after seven optimization cycles but the requirement for increased gain is met in only one cycle. The final solution has a maximum side lobe level just slightly above the dashed line which represents the limiting level of  $G_0 - 30$  dB. The optimizer of reference 17 will tolerate a moderate amount of constraint violation.

In terms of expansion or contraction of individual truss elements, a change in length of .066 inches seems very small. However, as seen in figure 4d, these small changes in length are enough to reduce the rms surface error from a starting value of 0.42 inches to a final value of  $\lambda/50$  or 0.17 inches and to produce a significant improvement in EM performance.

Figure 5 illustrates the change in antenna radiation patterns as a result of the optimization procedure. Figure 5 represents relative power as a function of  $\theta$  for two selected values of  $\phi$ . The final patterns are shaded black so that they can be compared to the original patterns which are white. The dashed line indicates the acceptable limit on side lobe levels. Notice that the side lobe levels are reduced for most values of  $\theta$  and  $\phi$ . However, the most significant effect of the optimization procedure is to narrow the main beam. It is anticipated that this amount of improvement in EM performance will have a significant effect on the accuracy of radiometer measurements.

#### Alternate Methods

The conventional approach to antenna shape control, (e.g. reference 3), is to use rms surface error as the sole criterion for improvement in the reflector surface geometry. In this section, the advantages and disadvantages of including EM performance criteria are explored.

The optimization procedure proposed in this paper can easily be repeated without EM calculations. The optimization problem becomes:

$$\begin{aligned} &\text{minimize} && \beta && (6) \\ &\text{subject to} && |\Delta l_i| \leq \beta && i=1,2, \dots, 48 \\ &&& \text{rms} \leq \lambda/50 \end{aligned}$$

This version of the optimization procedure can be completed very quickly because evaluation of equations (1-2) is trivial compared to evaluating antenna performance. Figure 6 compares the antenna patterns produced by the rms-limited procedure with the antenna patterns of the uncorrected antenna. Notice that there is very little improvement and that many of the side lobe levels exceed the limiting value. Clearly, simply reducing the rms surface error does not guarantee acceptable antenna performance. On the other hand, figure 4 indicates that the full optimization procedure reduces rms first and then satisfies side lobe limits. This suggests that the rms-limited procedure may provide an efficient way to calculate a good initial guess at the solution set possibly leading to faster convergence.

Another possible solution to antenna shape control is to strictly minimize rms error without regard to actuator cost. The set of actuator inputs which minimize rms is found by solving a set of simultaneous equations given in equation (3). This method is computationally efficient but it results in a  $\Delta l_{max}$  value which is more than 30 times larger than that of either previous method.

Table 1 provides a more complete comparison between the characteristics of the antenna reflector before and after each antenna correction method. The results should be compared to the required limits on side lobe level ( $SLL \leq G_0 - 30$  dB), gain ( $G \geq G_0 - .3$  dB) and rms distortion ( $rms \leq .17$ ).

Table 1 Results of Antenna Optimization

Optimization Method	SLL (wrt $G_0$ )	G (wrt $G_0$ )	rms in.	$\Delta l_{max}$ in.
none	-22.7	-.64	.418	0.
full	-29.7	-.11	.168	.066
rms-limited	-25.9	-.14	.172	.051
minimum rms required	-31.5	-.02	.067	2.200
	-30.0	-.30	.169	---

#### Refined Electromagnetic Analysis

As mentioned previously, the EM analysis during the optimization procedure calculates side lobe levels at only four azimuth angles. There is a real concern that reducing side lobe levels in four discrete directions

(i.e.  $\phi=0^\circ, 45^\circ, 90^\circ, 135^\circ$ ) simply allows side lobes levels to increase in other directions. This question can be addressed by performing a more detailed EM analysis of the optimized antenna and comparing it to a similar analysis of the unoptimized antenna. In this detailed analysis the relative power is calculated at 41 values of  $\theta$  and 41 values of  $\phi$  and presented in the form of a contour plot.

Figure 7 contains such contours for the original uncorrected antenna (see 7a), the full optimization solution (7b) and the rms-limited solution (7c) and the minimum rms solution (7d). Levels which are higher than -20 dB (wrt  $G_0$ ) are shaded black. Levels which are between -20 dB

and -25 dB are shaded dark gray. Levels which are between -25 dB and -30 dB are shaded light gray.

If the full optimization procedure was perfectly successful then all of the shaded areas in figure 7b would remain in the main beam region defined by a circle of radius  $\theta_0$ . In other words, all relative power levels outside the main beam would be at least 30 dB below  $G_0$ . By this criteria, the full optimization solution is not perfectly successful. However, the improvement between the uncorrected antenna and the corrected antenna is very significant. Additional improvement may be possible by using more than four azimuthal angles to define the side lobe level.

In contrast with the good results of the full optimization, the rms-limited optimization shows little improvement over the uncorrected antenna. Comparison of figures 7a and 7c verifies that simply improving the surface accuracy does not guarantee improvement of EM performance.

As expected, the contour which corresponds to the minimum rms surface distortion (see figure 7d) is the best. However, the difference between the contours in figures 7b and 7d is not very significant. It is questionable whether this small improvement justifies the increased actuator effort required to attain it.

#### Concluding Remarks

This paper described the development of an integrated structural-electromagnetic optimization procedure for shape control of orbiting large space antenna reflectors. The procedure employs standard finite element structural analysis, aperture integration EM analysis and constrained optimization techniques to predict a set of actuator inputs which will improve antenna performance while minimizing applied control effort. The procedure is tested for a 55-meter tetrahedral truss antenna design which has a surface distortion caused by length errors in individual members of the truss. It is shown that the current procedure converges to a much better set of actuator inputs than the traditional approach based on rms surface distortion constraints.

The procedure described in this paper is applicable to a wide variety of large space antenna concepts. The only assumption is that the original surface distortion is precisely known at a discrete number of surface locations and that the change in this distortion for a prescribed change in actuator inputs can be predicted. All alternative procedures make equivalent assumptions. The quality of the optimum design can be improved by improving the finite element model of the structure, by increasing the number of discrete points used to describe the surface and by increasing the number of azimuth angles used to define side lobe level.

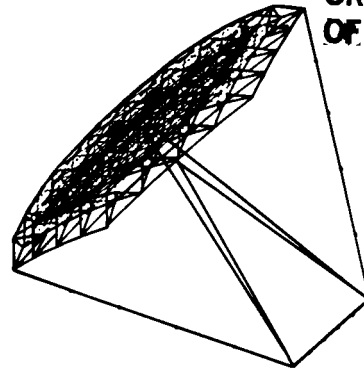
It is concluded that an integrated structures-electromagnetic optimization procedure is highly desirable for static shape

control of large space antennas. Indirect approaches which infer antenna performance from rms distortion may be unreliable and can use considerably more control effort than necessary.

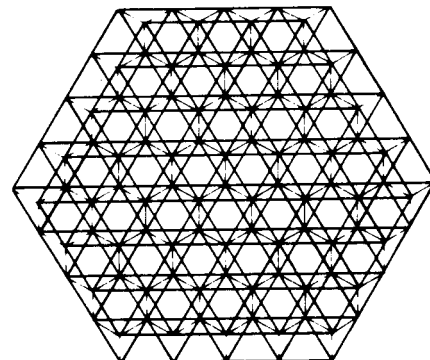
#### References

1. Lightner, E. B.: Large Space Antenna Systems Technology-1982. NASA CP-2269, 1983.
2. Anon.: Requirements, Design, and Development of Large Space Antenna Structures. AGARD Report R-676, May 1980.
3. Wright, R. L. (editor): The Microwave Radiometer Spacecraft - A Design Study. NASA RP-1079, December 1981.
4. Keafer, L. S. and Harrington, R. F.: Radiometer Requirements for Earth-Observation Systems Using Large Space Antennas. NASA RP-1101, June 1983.
5. Ruze, J.: Antenna Tolerance Theory - A Review Process of IEEE. Vol. 54, No. 4, April 1966, pp. 633-640.
6. Adelman, H. M.; and Padula, S. L.: Integrated Thermal Structural Electromagnetic Design Optimization of Large Space Antenna Reflectors. NASA TM-87713, June 1986.
7. Steinbach, Russell E.; and Winegar, Steven R.: Interdisciplinary Design Analysis of a Precision Spacecraft Antenna. AIAA Paper No. 85-0804.
8. Shu, C. F.; and Chang, M-H.: Integrated Thermal Distortion Analysis for Satellite Antenna Reflector. AIAA Paper No. 84-0142. Presented at AIAA 22nd Aerospace Science Meeting, Reno, NV, January 9-12, 1984.
9. Clark, S. C.; and Allen, G. E.: Thermo-Mechanical Design and Analysis System for the Hughes 76-inch Parabolic Antenna. AIAA Paper No. 82-0864. Presented at AIAA ASME 3rd Joint Thermophysics, Fluids, Plasma and Heat Transfer Conference, St. Louis, MO, June 7-11, 1982.
10. Greene, William H.: Effects of Random Member Length Errors on the Accuracy and Internal Loads of Truss Antennas. Journal of Spacecraft and Rockets, Vol. 22, No. 5, Sept-Oct 1985, pp. 554-559.
11. Haftka, R. T.; and Adelman, H. M.: An Analytical Investigation of Shape Control of Large Space Structures by Applied Temperatures. AIAA Journal, Vol. 23, No. 3, March 1985, pp. 450-457.
12. Haftka, R. T.; and Adelman, H. M.: Selection of Actuator Locations for Static Shape Control of Large Space Structures by Heuristic Integer Programming. In Advances and Trends in Structures and Dynamics. Edited by Noor and Hayduk, Pergamon Press, New York, 1985, pp. 575-582.
13. Whetstone, W. D.: EISI-EAL Engineering Analysis Language Reference Manual. Engineering Information Systems, Inc., San Jose, CA, 1983.
14. Rudduck, R.C.; and Chang, Y. C.: Numerical Electromagnetic Code - Reflector Antenna Code - NEC-REF (version 2) Part I: User's Manual. Report 712242-16, The Ohio State University ElectroScience Laboratory, Department of Electrical Engineering; Prepared under Contract N00123-79-C-1469 for Naval Regional Procurement Office, December 1982.
15. Bailey, M. C.: Hoop Column and Tetrahedral Truss Electromagnetic Tests. Presented at First NASA/DOD CSI Technology Conference, Norfolk, VA, November 18-21, 1986.
16. Crosswell, W. F. and Bailey, M. C.: Radiometer Antennas. Chapter 31, Antenna Engineering Handbook. Edited by Johnson and Jasik. McGraw-Hill Book Company, 1984.
17. Vanderplaats, G. N.: CONMIN - A FORTRAN Program for Constrained Function Minimization - User's Manual. NASA TMX#62282, August 1973.

ORIGINAL PAGE IS  
OF POOR QUALITY

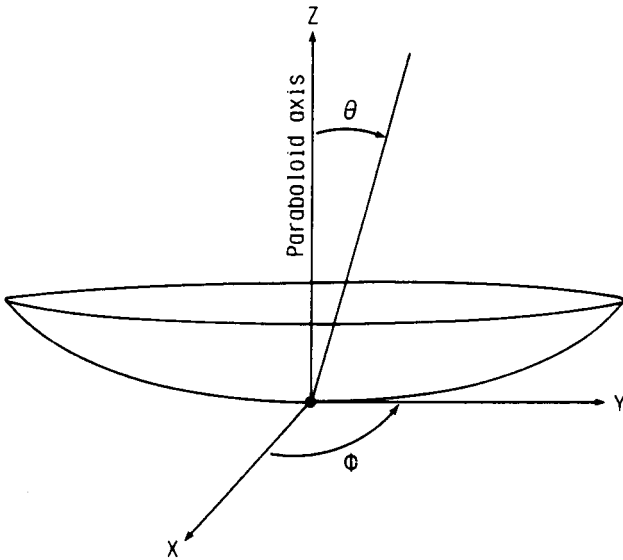


(a) Reflector antenna configuration.



(b) Finite element model.

Fig. 1 Geometry for radiometer antenna.



(c) Cartesian and cylindrical polar coordinate systems.

Fig. 1 Continued.

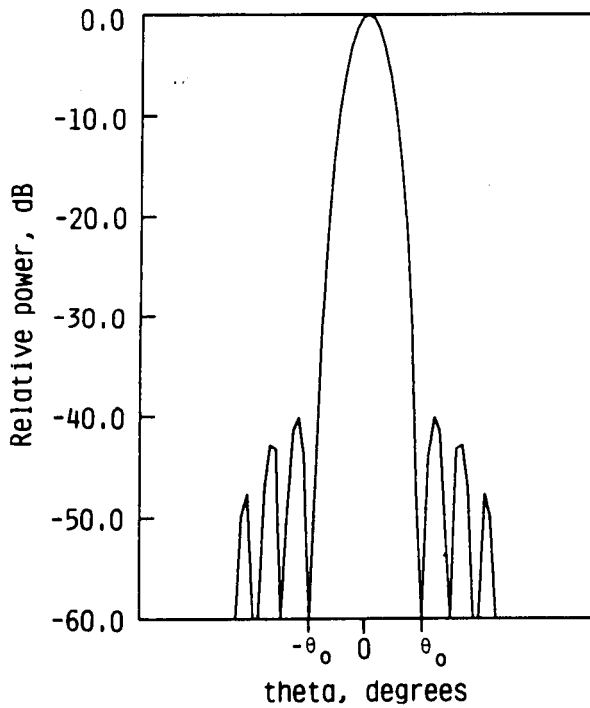
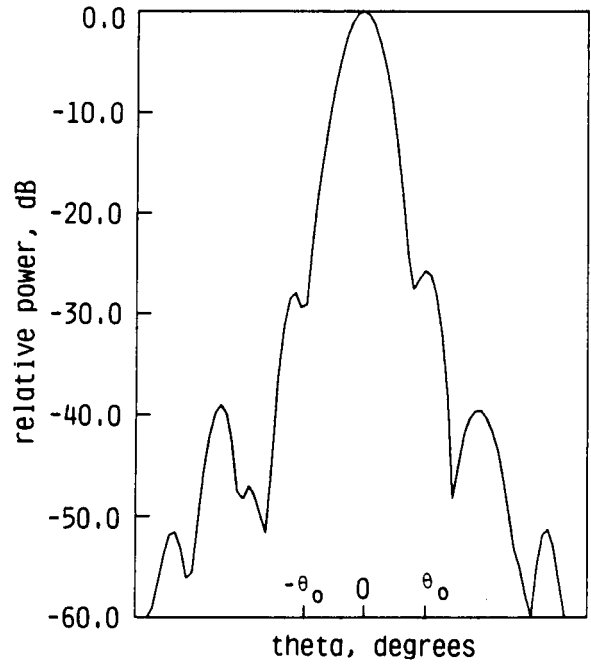
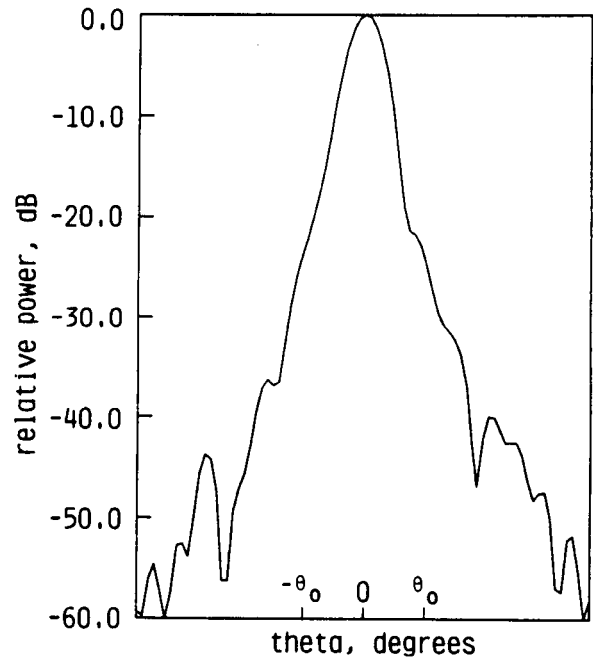


Fig. 2 Typical electromagnetic radiation pattern assuming undistorted reflector surface.



(a)  $\phi = 45$  degrees.

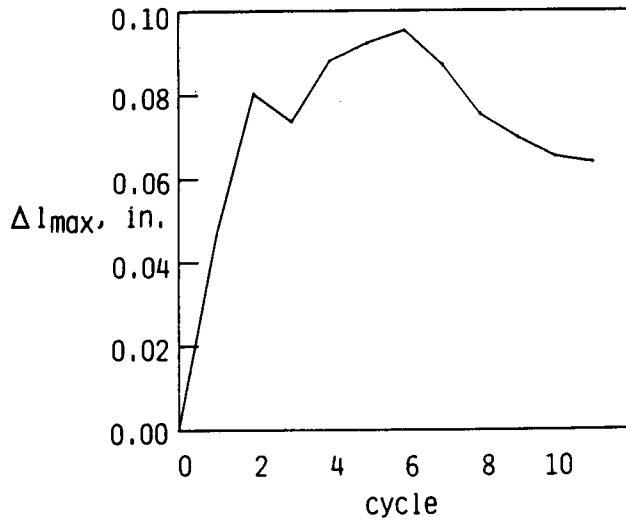
Fig. 3 Typical EM radiation patterns for randomly distorted reflector surface.



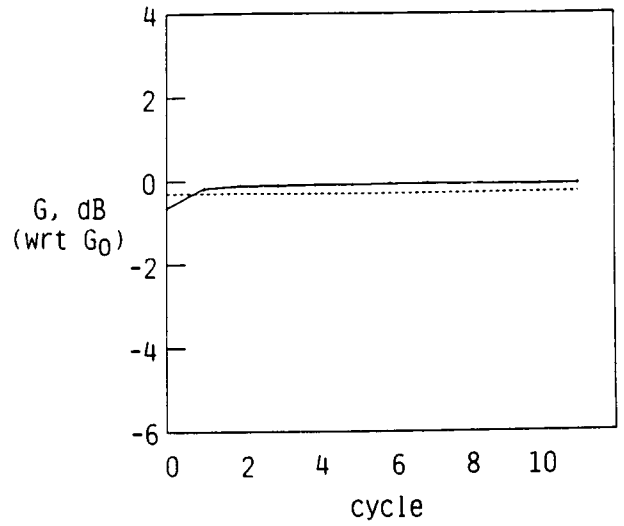
(b)  $\phi = 135$  degrees.

Fig. 3 Continued.

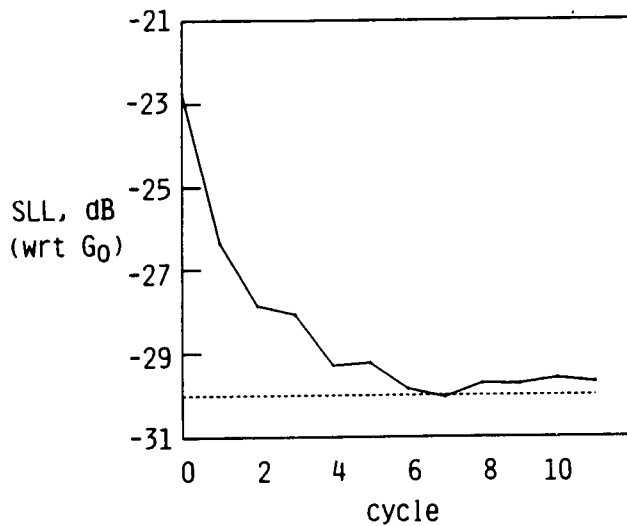




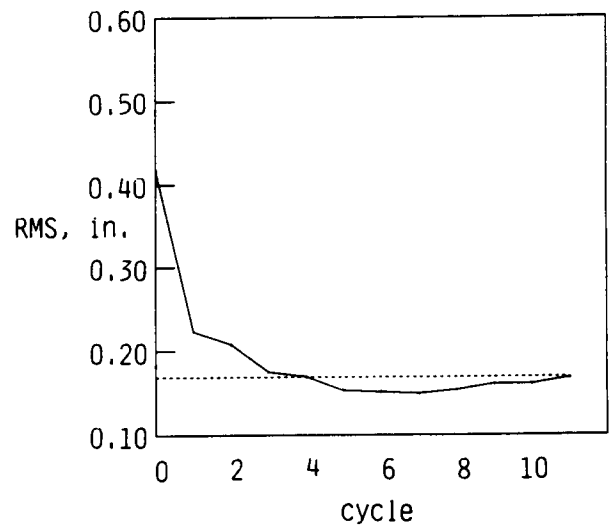
(a) Change in maximum actuator length with optimization cycle.



(c) Improvement in maximum power density (gain) with optimization cycle. (---- required level)

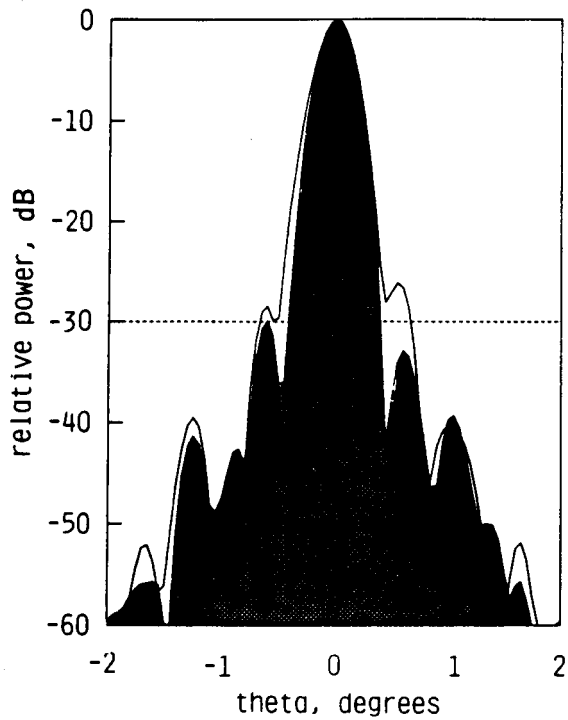


(b) Reduction in maximum side lobe level with optimization cycle. (---- allowable level)



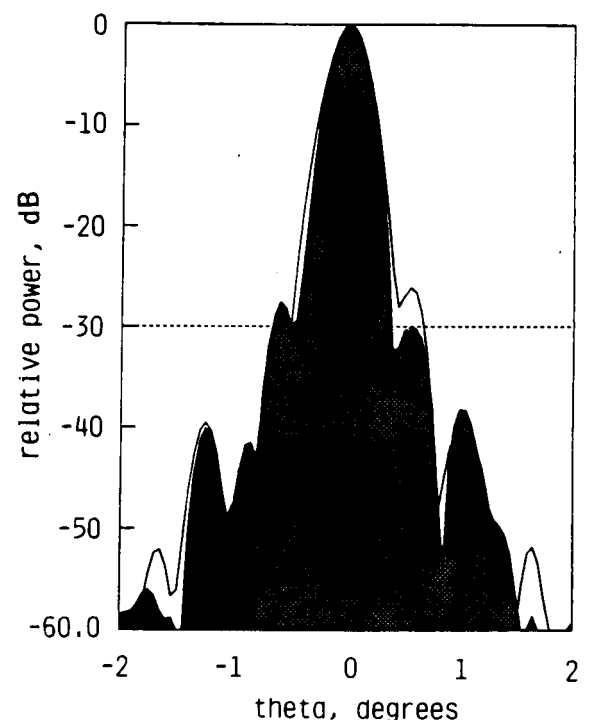
(d) Reduction in rms surface error with optimization cycle. (---- allowable level)

Fig. 4 Convergence history of the optimization procedure.



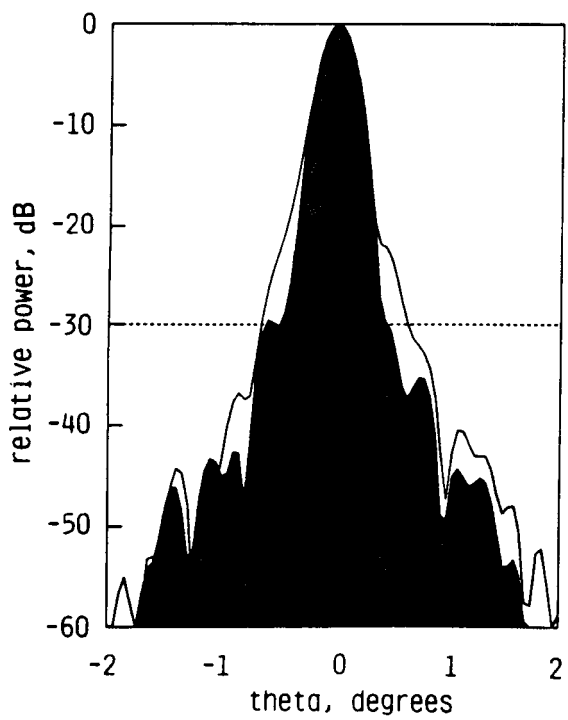
(a)  $\phi = 45$  degrees.

Fig. 5 Comparison of EM radiation patterns before (white) and after (dark) full optimization. (---- allowable side lobe level)



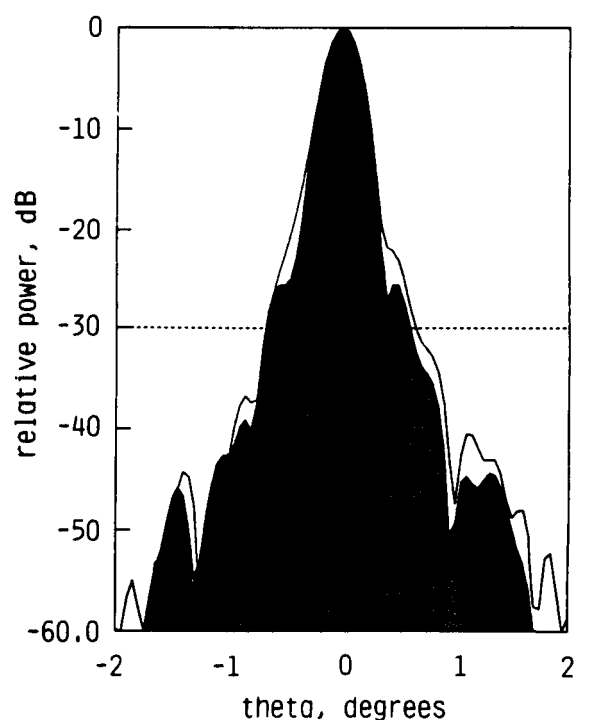
(a)  $\phi = 45$  degrees.

Fig. 6 Comparison of EM radiation patterns before (white) and after (dark) rms-limited optimization. (---- allowable side lobe level)



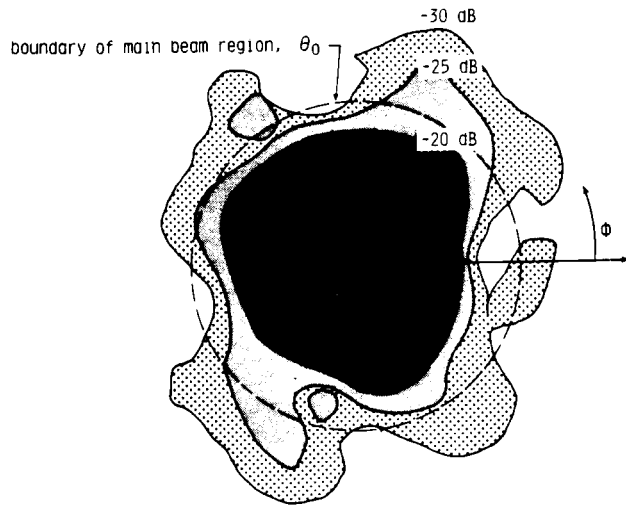
(b)  $\phi = 135$  degrees.

Fig. 5 Continued.

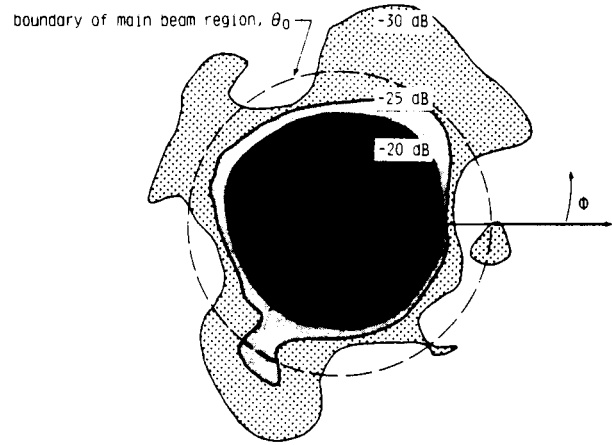


(b)  $\phi = 135$  degrees.

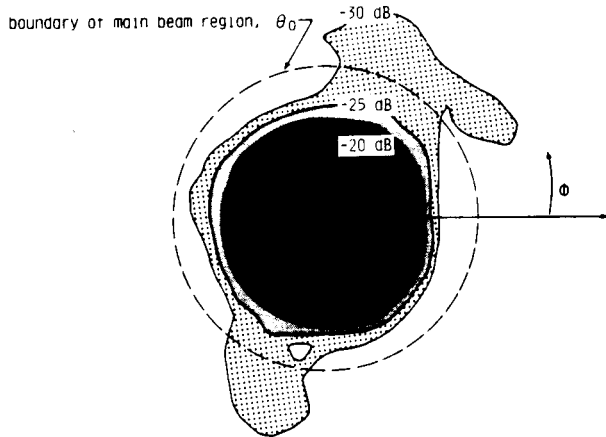
Fig. 6 Continued.



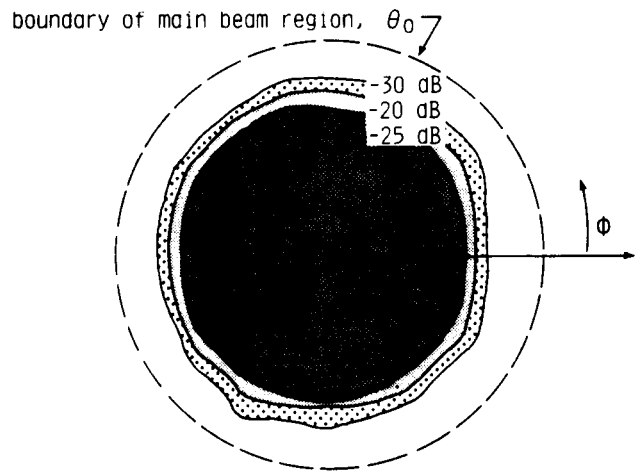
(a) Power level contours before optimization.



(c) Power level contours after rms-limited optimization.



(b) Power level contours after full optimization.



(d) Power level contours for minimum rms surface distortion.

Fig. 7 Predicted relative power levels on any plane normal to paraboloid axis.

1. Report No. NASA TM-89110		2. Government Accession No.		3. Recipient's Catalog No.	
4. Title and Subtitle Integrated Structure Electromagnetic Optimization of Large Space Antenna Reflectors				5. Report Date February 1987	
				6. Performing Organization Code 506-43-41-01	
7. Author(s) Sharon L. Padula, Howard M. Adelman, and M. C. Bailey				8. Performing Organization Report No.	
9. Performing Organization Name and Address  NASA Langley Research Center Hampton, VA 23665				10. Work Unit No.	
				11. Contract or Grant No.	
12. Sponsoring Agency Name and Address  National Aeronautics and Space Administration Washington, DC 20546				13. Type of Report and Period Covered Technical Memorandum	
				14. Sponsoring Agency Code	
15. Supplementary Notes  Presented at AIAA/ASME/ASCE/AHS 28th Structures, Structural Dynamics and Materials Conference, Monterey, CA, April 6-8, 1987. AIAA Paper No. 87-0824-CP.					
16. Abstract  The requirements for extremely precise and powerful large space antenna reflectors have motivated the development of a procedure for shape control of the reflector surface. A mathematical optimization procedure has been developed which improves antenna performance while minimizing necessary shape correction effort. In contrast to previous work which proposed controlling the rms distortion error of the surface thereby indirectly improving antenna performance, the current work includes electromagnetic (EM) performance calculations as an integral of the control procedure. The application of the procedure to a radiometer design with a tetrahedral truss backup structure demonstrates the potential for significant improvement. The results indicate the benefit of including EM performance calculations in procedures for shape control of large space antenna reflectors.					
17. Key Words (Suggested by Author(s)) Optimization methods Large space structures Space antennas Shape control			18. Distribution Statement  Unclassified - Unlimited Subject Category 18		
19. Security Classif. (of this report) Unclassified		20. Security Classif. (of this page) Unclassified		21. No. of Pages 11	22. Price A02